Probing the mobility of polymers grafted on cosmetic pigments using NMR and EPR spectroscopies

Lafon, Olivier[1*]; Vezin, Hervé[2]; Rankin, Andrew[3]; Trébosc, Julien[3]; Vallet, Alicia[4]; Takahashi, Tetsuya[5]

[1] Université de Lille, CNRS, Centrale Lille, Univ. Artois, UMR 8181 − UCCS – Unité de Catalyse et Chimie du Solide, 59000 Lille, France ; [2] Université de Lille, CNRS, UMR 8516-LASIRE, 59000 Lille, France; [3] Univ. Lille, CNRS, INRAE, Centrale Lille, Univ. Artois, FR 2638 - IMEC - Institut Michel-Eugène Chevreul, 59000 Lille, France ; [4] Univ. Grenoble Alpes, CEA, CNRS, Institut de Biologie Structurale (IBS), 71 avenue des Martyrs, 38044 Grenoble Cedex 9, France ; [5] Miyoshi Europe S.A.S., 5, rue Paul Rieupeyroux, 69800 St. Priest, France.

* Olivier Lafon, UCCS, avenue Mendeleïev, Bât. C7, CS 90108, 59652 Villeneuve d'Ascq Cedex, +333 74 95 13 12 and olivier.lafon@univ-lille.fr

Abstract

Background: Since 2017, regulatory actions have been taken at European Union level to limit the use of microplastics in products in order to improve the protection of environment. In particular, all cosmetic pigments containing polymers will considered as microplastics according to the definition added to REACH and will be banned from manufacture and sale in 2026. A possible exclusion is the case of nonsolid polymer. Therefore, it is crucial to determine the mobility of siloxane polymers grafted on the surface of pigments.

Methods: We investigated herein the mobility of either polydimethylsiloxane (PDMS), also called dimethicone, or polymethylhydrosiloxane (PMHS), also called methicone, grafted on the surface of TiO_2 pigments using EPR as well as ^1H and ^{13}C solid-state NMR spectroscopies.

Results: These studies indicate that both polymers contain rigid and mobile segments. Nevertheless, most segments of PDMS chains are mobile and the polymer remains almost entirely in liquid-like state. Conversely, the majority of PMHS segments are rigid owing to the formation of Ti−O−Si bonds since one third of SiH groups of PMHS chains react with hydroxyl groups at the surface of TiO_2 particles.

Conclusion: The TiO$_2$ pigments treated by PDMS must not be considered as microplastics according to the REACH definition, since the polymer chains remain largely in liquid-like state. Conversely the pigments treated by PMHS results in the formation of microplastics.

Keywords: microplastics; mobility; polymers; NMR; EPR

Introduction

In 2017, the European Commission asked the European Chemicals Agency (ECHA) to evaluate scientific evidence for EU-level regulatory action on microplastics intentionally added to products as a precautionary measure against environmental hazard concerns. In response, ECHA presented a Q & A on July 10, 2019 as a proposal for the definition of microplastics in general [1]. Furthermore, on August 22, 2019, the detailed definition of microplastics was added to REACH [2]. At the same time, at the request of ECHA, the Risk Assessment Committee (RAC) and the Socio-Economic Analysis Committee (SEAC) submitted a written opinion on June 11, 2020 [3].

Some of the cosmetic pigments on the market today are surface-treated with polymers to improve "feel" and water resistance (sweat resistance). According to the definition of microplastics added to REACH, all solid pigments containing polymers will be defined as microplastics and will be banned from manufacture and sale in 2026.

There are two exclusions in this current provision: "Polymer content is 1% w/w or less and does not cover the entire surface of the pigment" or "Polymer is not solid". The surface treatment of cosmetic pigments with siloxane polymer does not cover the entire surface of the pigment, but it requires use of 1% or more to guarantee its functional effect. In other words, the former exclusion item cannot be applied.

The siloxane polymers, which are the surface treatment agents, are completely liquid before being treated on the pigment. Nevertheless, it is not yet known whether the polymer remains in a liquid-like state after the grafting on the pigment. Considering the origin of the regulation is related to environmental impact mitigation, it is crucial to determine whether the polymer in the surface-treated pigment is in a liquid or solid state, and hence, the surface treatment of pigments with polymers results in the formation of microplastics.

To this end, we treated herein TiO_2 pigments with either polydimethylsiloxane (PDMS), also known as dimethicone, or polymethylhydrosiloxane (PMHS), also known as methicone, which form different types of covalent bonds with the pigment surface and investigated the mobility of polymer chains using electron paramagnetic resonance (EPR) and solid-state nuclear magnetic resonance (NMR) spectroscopies.

Materials and Methods.

EPR

EPR experiments were performed using an X-band spectrometer operating at 9.81 GHz with respectively 100 kHz and 1 G for modulation frequency and amplitude. The microwave power was set to 1 mW to avoid saturation. The EPR spectra were simulated using EasySpin software [4,5].

Solution-State NMR

One-dimensional (1D) ^1H and ^{13}C NMR experiments were recorded at a static magnetic field, $B_0 = 9.4$ T, *i.e*., Larmor frequencies of 400 MHz for ^1H and 100 MHz for ^{13}C and 300 K with a standard bore magnet equipped with Bruker AVANCE NEO NMR console and a 5 mm inverse triple-resonance $^1H/^{13}C/X$ (TBI) probe. $[^2H_6]$-acetone in a small internal tube was used for sample locking. ^1H and ^{13}C isotropic chemical shifts were referenced with respect to a solution of 1% tetramethylsilane (TMS) in $CDCl_3$ using the residual solvent peak (methanol) as a secondary reference.

The ^1H NMR spectrum was acquired by averaging 16 transients separated by a recycle interval of 1 s, using a single-pulse experiment. A $\pi/2$ radiofrequency (rf) pulse of 9.39 μs with nutation frequency $\nu_1 \approx 26.6$ kHz was used. ^1H longitudinal and transverse relaxation time constants, $T_1(^1H)$ and $T_2(^1H)$, were measured using inversion-recovery and Carr-Purcell Meiboom-Gill (CPMG) sequences, respectively.

The ^{13}C NMR spectrum was acquired by averaging 256 transients separated by a recycle interval of 2 s, using a *J*-modulated spin-echo experiment using rf pulses with a nutation frequency $\nu_1 \approx 16.7$ kHz on ^{13}C channel and power-gated decoupling with $\nu_1 \approx 2.8$ kHz on ^1H channel.

Solid-State NMR

1D ^{1}H, ^{13}C, ^{1}H $\rightarrow$ ^{13}C cross-polarization under magic-angle spinning (CPMAS) and ^{1}H $\rightarrow$ ^{13}C *J*-RINEPT [6] experiments were recorded at B_0 = 9.4 T *i.e.*, Larmor frequencies of 400 MHz for ^{1}H and 100 MHz for ^{13}C and room temperature on a wide bore magnet equipped with Bruker AVANCE III NMR console and Bruker double- resonance ^{1}H/X 4 mm magic-angle spinning (MAS) probe. Powdered samples were packed into 4 mm outer diameter zirconia rotors with Kel-F drive caps and spun at a MAS rate, ν_R = 12.5 kHz. ^{1}H and ^{13}C isotropic chemical shifts were referenced with respect to a solution of 1% tetramethylsilane (TMS) in CDCl$_3$ using the CH$_2$ group resonance of a solid sample of adamantane at 1.735 ppm (^{1}H) or 37.77 ppm (^{13}C) as a secondary reference.

^{1}H NMR spectra were acquired by averaging 128 transients separated by a recycle interval of 5 s, using the DEPTH pulse sequence for probe background suppression [7], with $\nu_1 \approx$ 89 kHz. $T_1(^1$H$)$ relaxation time and the time constant associated to the homogeneous contribution to dephasing, T_2'(^{1}H), were measured using saturation-recovery and Hahn echo sequences, respectively.

^{13}C NMR spectra were acquired by averaging 896 transients separated by a recycle interval of 60 s, using single-pulse experiments. A π/2 pulse of 3 μs with $\nu_1 \approx$ 83 kHz was used. SPINAL ^{1}H decoupling [8] with $\nu_1 \approx$ 20 kHz was applied during the acquisition period.

^{1}H $\rightarrow$ ^{13}C CP MAS NMR experiments were acquired with an initial ^{1}H π/2 pulse lasting 2.8 μs with $\nu_1 \approx$ 89 kHz, followed by CP contact times τ_{CP} = 2.5 or 25 ms. During the CP transfer, the rf nutation frequency on the ^{13}C channel was constant and equal to 38 kHz, while the ^{1}H nutation frequency was linearly ramped from 45 to 50 kHz. Spectra were recorded using recycle intervals equal to 1.3$T_1(^1$H$)$ to maximize the sensitivity.[9] SPINAL ^{1}H decoupling[8] with $\nu_1 \approx$ 6 kHz was applied during acquisition.

^{1}H$\rightarrow$^{13}C *J*-RINEPT NMR experiments were acquired with ^{1}H π/2 and π pulses lasting 2.8 μs and 5.6 μs, respectively. ^{13}C π/2 and π pulses lasted 3 μs and 6 μs, respectively. Defocusing and refocusing delays of τ_1 = 2.08 ms and τ_2 = 0.69 ms were used. Spectra were recorded using recycle intervals equal to 1.3$T_1(^1$H$)$, and were the result of averaging 19456 or 25600 transients. SPINAL ^{1}H decoupling with $\nu_1 \approx$ 6 kHz was applied during the acquisition period.

Data processing and analysis was performed with the Bruker TopSpin, DMFit and Gnuplot software programs.

Results.

EPR

We first used TEMPO nitroxide radicals as a probe of the polymer chains mobility at the surface of the pigments. For that purpose, we first dissolved TEMPO radicals in a sample of TiO_2 pigment functionalized with PDMS chains. The obtained EPR spectrum shown in Figure 1a is dominated by a narrow triplet due to the hyperfine coupling with ^{14}N nucleus. This spectrum can be simulated with a rotational correlation time of TEMPO probe, $\tau_c = 3.1$ ns. To check the influence of the grafting of PDMS chains on the surface of TiO_2 pigment, we also recorded the EPR spectrum of TEMPO radicals dissolved in a physical mixture of PDMS and TiO_2 pigment. This spectrum shown in Figure 1b also exhibits a single triplet with narrower components than for the grafted PDMS. This triplet can be simulated with $\tau_c = 1.8$ ns. Conversely the EPR spectrum of TEMPO radicals dissolved in a sample of TiO_2 pigment functionalized by PMHS chains, displayed in Figure 1c, exhibits, beside the narrow triplet, a broad triplet owing to the anisotropic hyperfine coupling with ^{14}N nucleus. This spectrum was simulated with $\tau_c = 6.7$ ns, a *z*-component of the ^{14}N hyperfine tensor, $2A_{zz} = 34.0$ G, and a relative integrated intensity $II/II_{tot} = 48\%$ for the narrow triplet, instead of $\{\tau_c, 2A_{zz}, II/II_{tot}\} = \{52$ ns, 61.9 G, $52\%\}$ for the broad triplet. Hence, the TEMPO probe partitions in two types of PMHS domains: (i) some mobile chains yielding the narrow triplet and (ii) some rigid domain producing the broad triplet. Nevertheless, the correlation time and hence, the mobility of TEMPO radicals are lower in the mobile domain of PMHS than in the PMDS grafted on the surface of TiO_2 particles.
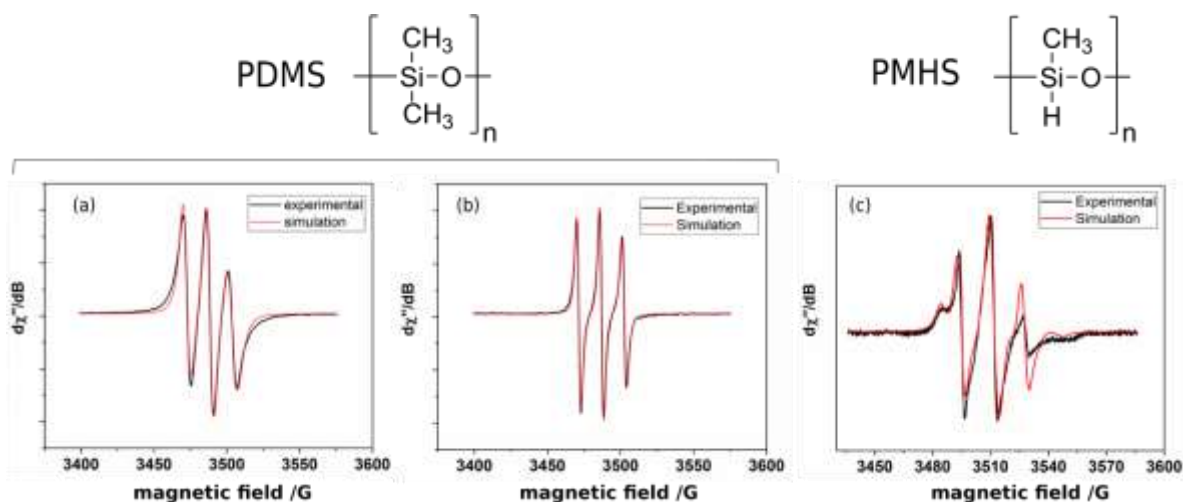
Figure 1. Experimental (black) and simulated (red) EPR spectra of TEMPO radicals dissolved in samples of (a) TiO_2 particles functionalized with PDMS, (b) a physical mixture of TiO_2 particles and PDMS, (c) TiO_2 particles functionalized with PMHS. The structures of PDMS and PMHS polymers are shown as insets on the top of the figure.

^{1}H solid-state NMR

The 1D ^{1}H MAS spectrum of TiO_2 particles functionalized with PDMS, shown in Figure 2 in red, is dominated by a narrow peak resonating at −0.1 ppm assigned to the methyl groups of PDMS chains. Furthermore, this spectrum exhibits a broad signal at 4.5 ppm assigned to water molecules adsorbed on the surface of TiO_2 particles [10]. The 1D ^{1}H MAS spectrum of TiO_2 particles functionalized with PMHS, displayed in Figure 2 in blue, exhibits two major ^{1}H signals: a narrow and intense peak resonating at 0.0 ppm assigned to the methyl group of PMHS chains as well as a weaker signal at 4.6 ppm assigned to SiH protons [11]. This quantitative spectrum was simulated using dmfit software [12]. This simulation [not shown] indicates that the integrated intensity of CH_3 signals is 4.5 times larger than that of SiH signals for TiO_2 particles functionalized with PMHS, instead of 3 for the pristine PMHS polymer. This result shows that one third of SiH groups of PMHS reacts with surface hydroxyl groups of TiO_2 particles to form Si−O−Ti covalent bonds.

Furthermore, the methyl signal of PMHS is significantly broader than that of PDMS. This broadening betrays larger ^{1}H-^{1}H dipolar couplings, and hence, lower mobility of PMHS chains compared to the PDMS polymer. This result is consistent with the average T_2'(^{1}H) values, which are equal to 9.2 and 2.4 ms for PDMS and PMHS methyl groups, respectively. In contrast, the T_1(^{1}H) values of the methyl groups of PDMS and PMHS polymers grafted on the surface of TiO_2 particles are equal to 0.78 and 0.91 s, respectively and hence, does not

differ significantly since the longitudinal relaxation of the methyl protons is dominated by the rotation of the methyl group.
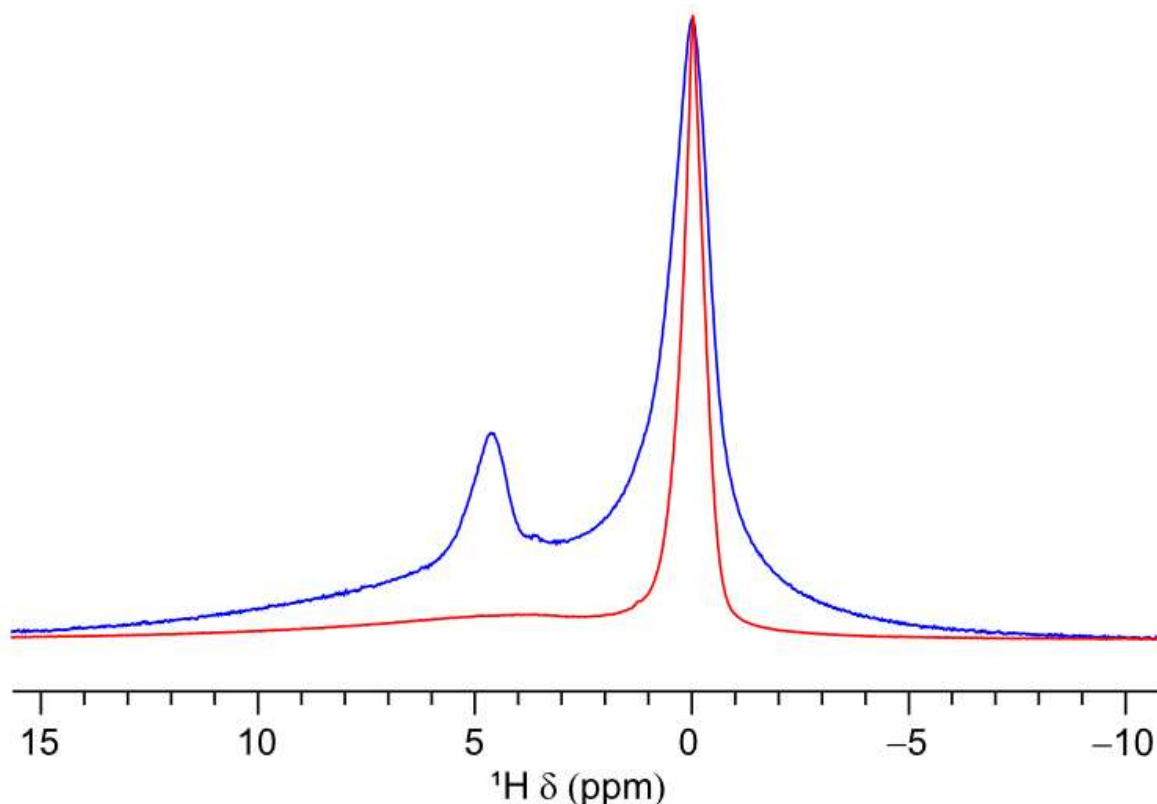

Figure 2. 1D ^{1}H MAS NMR spectra of TiO$_2$ particles functionalized with PDMS (red) and TiO$_2$ particles functionalized with PMHS (blue) acquired at $B_0 = 9.4$ T with $\nu_R = 12.5$ kHz.

^{13}C solid-state NMR

The mobility of polymer chains grafted on the surface of TiO$_2$ particles was also probed by recording and comparing ^{13}C NMR spectra acquired with ^{1}H → ^{13}C CPMAS and *J*-RINEPT polarization transfers as well as single-pulse sequence. This approach has been utilized to identify rigid and mobile molecular segments in several systems, including lipid membranes [13], amyloid fibrils [14], surfactants [15], liquid crystals [16] and the stratum corneum, which is the outermost layer of skin [17,18]. A signal in CPMAS spectrum can be observed for rigid molecular segments with slow and/or anisotropic motions since the ^{1}H → ^{13}C CP transfer is mediated by ^{1}H-^{13}C dipolar couplings, which are averaged out by fast isotropic reorientation. Conversely, the ^{1}H → ^{13}C *J*-RINEPT experiment allows the observation of mobile segments since the ^{1}H transverse magnetization rapidly decays under ^{1}H-^{1}H dipolar couplings during the defocusing delay of *J*-RINEPT experiment. Segments with rapid but anisotropic motions produce signals in both CPMAS and *J*-RINEPT spectra.

The quantitative ^{13}C single-pulse NMR experiment allows the observation of all molecular segments and gives signal integrated intensities proportional to the concentrations of the different segments.

Figure 3a compares the ^{1}H $\rightarrow$ ^{13}C CPMAS and *J*-RINEPT NMR spectra as well as the quantitative ^{13}C single-pulse NMR spectrum of TiO$_2$ particles functionalized width PDMS. The *J*-RINEPT and single-pulse NMR spectra are almost identical. This result indicates that most PDMS segments are highly mobile and are in liquid-like state. Nevertheless, ^{1}H $\rightarrow$ ^{13}C CPMAS spectra exhibits some signal. Hence, a small fraction of PDMS segments are subject rigid or subject to anisotropic motions. Furthermore, the CPMAS spectra are broader than the *J*-RINEPT signal since the ^{13}C nuclei in the rigid segments exhibits a distribution of local environments and hence, of ^{13}C isotropic chemical shifts, whereas for the mobile segments, these differences in local environment are averaged out by the molecular motions. The ^{1}H $\rightarrow$ ^{13}C CPMAS spectrum acquired with τ_{CP} = 25 ms is narrower than that acquired with τ_{CP} = 2.5 ms since the most rigid segments exhibiting the broadest signals are subject to the larger ^{1}H-^{1}H dipolar interactions and their spin-locked ^{1}H magnetization decays faster during the ^{1}H $\rightarrow$ ^{13}C CP transfer.
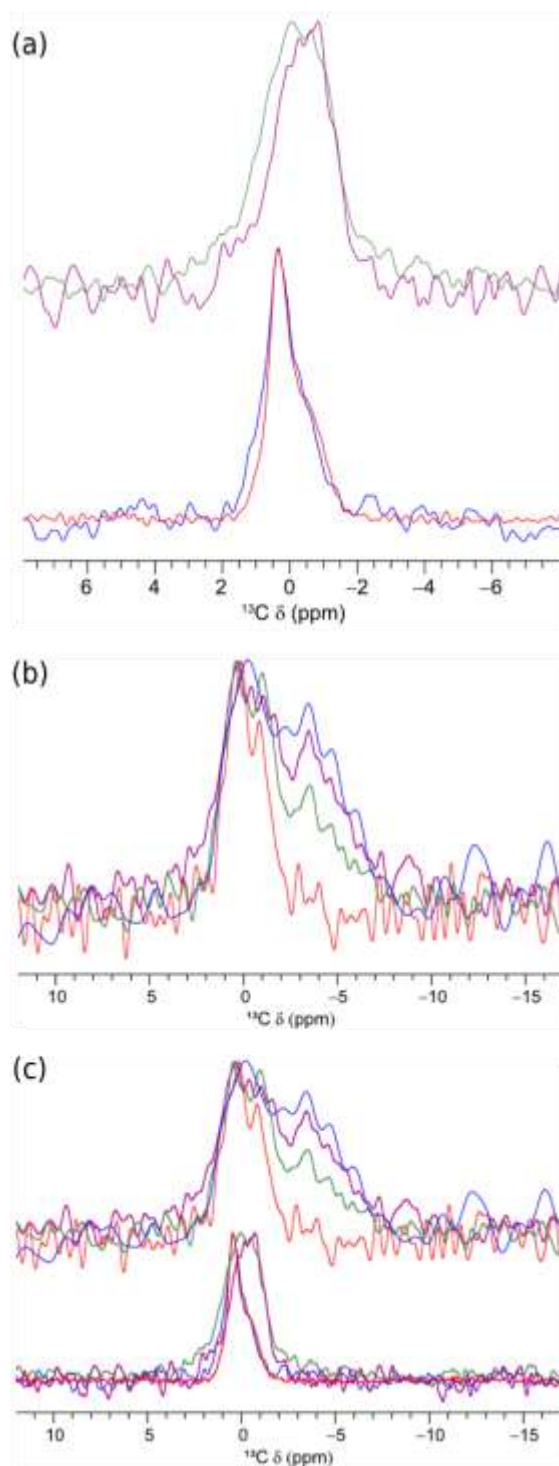
Figure 3. 1D ^{13}C MAS NMR spectra of (a) TiO_2 particles functionalized with PDMS and (b) TiO_2 particles functionalized with PMHS acquired at $B_0 = 9.4$ T with $\nu_R = 12.5$ kHz using $^1H \rightarrow {}^{13}C$ CPMAS with $\tau_{CP} = 2.5$ (green) or 25 ms (purple), or J-RINEPT (red) polarization transfers, or single-pulse sequence (blue). The spectra are displayed with different horizontal scales. (c) Comparison of the 1D ^{13}C MAS NMR spectra of panels (a) (bottom) and (b) (top) displayed with the same horizontal scale. In the three panels, the spectra are normalized to the same maximal intensity.

The Figure 3b displays the $^1H \rightarrow {}^{13}C$ CPMAS and *J*-RINEPT NMR spectra as well as the quantitative ^{13}C single-pulse NMR spectrum of TiO_2 particles functionalized with PMHS. All the spectra are broader than their counterparts for PDMS, as seen in Figure 3c, which indicates lower mobility in the PMHS with respect to PDMS. Furthermore, contrary to PDMS, the quantitative ^{13}C single-pulse NMR and $^1H \rightarrow {}^{13}C$ CPMAS spectra exhibit similar lineshapes. This observation indicates that the vast majority of PMHS segments is rigid. Nevertheless, PMHS chains exhibit $^1H \rightarrow {}^{13}C$ *J*-RINEPT signals, which shows the presence of a small fraction of mobile segments for this polymer.

Discussion

EPR as well as ^1H and ^{13}C solid-state NMR results show that PDMS and PMHS chains grafted on TiO_2 surfaces contain both mobile and rigid segments. Nevertheless, most of PDMS segments are mobile and remain in liquid-like state at room temperature, whereas the majority of PMHS segments are rigid and forms a solid fraction in the same conditions. This difference notably stems from the formation of Ti−O−Si links between TiO_2 surface and PMHS chains by reaction between one of third of their SiH groups and surface hydroxyl groups.

To the best of our knowledge, the mobility of PMHS polymers grafted on the surface of inorganic particles has not been reported in the literature. Conversely, the mobility of PDMS polymers grafted on one end or physically adsorbed on TiO_2 surface has been investigated using differential scanning calorimetry (DSC) and dielectric spectroscopy [19–22]. Furthermore, these techniques as well as solid-state NMR and computer simulations have been employed to probe the mobility of PDMS grafted or physically on silica surface [23–31]. These studies have demonstrated that the thickness of rigid PDMS layer on silica surface is about 1 nm [23,27,30]. This thickness was doubled in the case of TiO_2 surface owing to stronger interactions of PDMS with the surface [19,20]. This rigid layer produces $^1H \rightarrow {}^{13}C$ CPMAS signals seen in Figure 3a.

Conclusion.

We compared using EPR and ^1H and ^{13}C solid-state NMR spectroscopy the mobility of PDMS and PMHS chains grafted on the surface of TiO_2 particles used as pigments in cosmetics. Both polymers contain rigid and mobile segments. Nevertheless, for PDMS, the rigid segments only represent a small fraction, corresponding to a layer of a few nanometers

close to the TiO_2 surface, and most of the PDMS chains are mobile in a liquid-like state. Conversely, for PMHS, the majority of the segments are rigid. This difference notably stems from the formation of Ti−O−Si links between TiO_2 surface and PMHS chains. Proton solid-state NMR spectrum indicates that one third of SiH groups of PMHS chains have reacted with hydroxyl groups of TiO_2 surface. Therefore, TiO_2 particles functionalized with PDMS chains do not form microplastics according to the definition of REACH, whereas their counterpart with PMHS does.

Conflict of Interest Statement. Partial financial support was received from Miyoshi Europe S.A.S.

References.

[1] Restriction proposal on intentionally-added microplastics – questions and answers, European Chemicals Agency (ECHA), Helsinki, 2020.
[2] Annex to Annex XV Restriction Report, substance name: Intentionally Added Microplastics, version 1.2, European Chemicals Agency (ECHA), 2019.
[3] Opinion on an Annex XV dossier proposing restrictions on intentionally-added microplastics, Committee for Risk Assessment (RAC) Committee for Socio-economic Analysis (SEAC), 2020.
[4] S. Stoll, A. Schweiger, EasySpin, a comprehensive software package for spectral simulation and analysis in EPR., Journal of Magnetic Resonance (San Diego, Calif. : 1997). 178 (2006) 42–55. https://doi.org/10.1016/j.jmr.2005.08.013.
[5] S. Stoll, R.D. Britt, General and efficient simulation of pulse EPR spectra., Physical Chemistry Chemical Physics : PCCP. 11 (2009) 6614–25. https://doi.org/10.1039/b907277b.
[6] G.A. Morris, R. Freeman, Enhancement of nuclear magnetic resonance signals by polarization transfer, J. Am. Chem. Soc. 101 (1979) 760–762. https://doi.org/10.1021/ja00497a058.
[7] D.G. Cory, W.M. Ritchey, Suppression of signals from the probe in bloch decay spectra, J. Magn. Reson. 80 (1988) 128–132.

[8] B.M. Fung, A.K. Khitrin, K. Ermolaev, An Improved Broadband Decoupling Sequence for Liquid Crystals and Solids, J. Magn. Reson. 142 (2000) 97–101. https://doi.org/DOI: 10.1006/jmre.1999.1896.

[9] M. Pons, M. Feliz, E. Giralt, Steady-State DQF-COSY Spectra Using a Variable Relaxation Delay, J. Magn. Reson. 78 (1988) 314–320.

[10] M.J. Torralvo, J. Sanz, I. Sobrados, J. Soria, C. Garlisi, G. Palmisano, S. Çetinkaya, S. Yurdakal, V. Augugliaro, Anatase photocatalyst with supported low crystalline TiO_2: The influence of amorphous phase on the activity, Applied Catalysis B: Environmental. 221 (2018) 140–151. https://doi.org/10.1016/j.apcatb.2017.08.089.

[11] B.G. Kim, J.-K. Moon, E.-H. Sohn, J.-C. Lee, J.-K. Yeo, Polysiloxanes containing alkyl side groups: synthesis and mesomorphic behavior, Macromol. Res. 16 (2008) 36–44. https://doi.org/10.1007/BF03218958.

[12] D. Massiot, F. Fayon, M. Capron, I. King, S. Le Calvé, B. Alonso, J.-O. Durand, B. Bujoli, Z. Gan, G. Hoatson, Modelling one- and two-dimensional solid-state NMR spectra, Magn. Reson. Chem. 40 (2002) 70–76.

[13] D.E. Warschawski, P.F. Devaux, Polarization Transfer in Lipid Membranes, Journal of Magnetic Resonance. 145 (2000) 367–372. https://doi.org/10.1006/jmre.2000.2135.

[14] M. Sackewitz, H.A. Scheidt, G. Lodderstedt, A. Schierhorn, E. Schwarz, D. Huster, Structural and Dynamical Characterization of Fibrils from a Disease-Associated Alanine Expansion Domain Using Proteolysis and Solid-State NMR Spectroscopy, J. Am. Chem. Soc. 130 (2008) 7172–7173. https://doi.org/10.1021/ja800120s.

[15] A. Nowacka, P.C. Mohr, J. Norrman, R.W. Martin, D. Topgaard, Polarization Transfer Solid-State NMR for Studying Surfactant Phase Behavior, Langmuir. 26 (2010) 16848–16856. https://doi.org/10.1021/la102935t.

[16] A. Nowacka, N.A. Bongartz, O.H.S. Ollila, T. Nylander, D. Topgaard, Signal intensities in ^1H–^{13}C CP and INEPT MAS NMR of liquid crystals, Journal of Magnetic Resonance. 230 (2013) 165–175. https://doi.org/10.1016/j.jmr.2013.02.016.

[17] S. Björklund, A. Nowacka, J.A. Bouwstra, E. Sparr, D. Topgaard, Characterization of Stratum Corneum Molecular Dynamics by Natural-Abundance 13C Solid-State NMR, PLOS ONE. 8 (2013) e61889. https://doi.org/10.1371/journal.pone.0061889.

[18] Q.D. Pham, D. Topgaard, E. Sparr, Tracking solvents in the skin through atomically resolved measurements of molecular mobility in intact stratum corneum, Proceedings of the National Academy of Sciences. 114 (2017) E112–E121. https://doi.org/10.1073/pnas.1608739114.

[19] P. Klonos, A. Panagopoulou, L. Bokobza, A. Kyritsis, V. Peoglos, P. Pissis, Comparative studies on effects of silica and titania nanoparticles on crystallization and complex segmental dynamics in poly(dimethylsiloxane), Polymer. 51 (2010) 5490–5499. https://doi.org/10.1016/j.polymer.2010.09.054.

[20] P. Klonos, A. Panagopoulou, A. Kyritsis, L. Bokobza, P. Pissis, Dielectric studies of segmental dynamics in poly(dimethylsiloxane)/titania nanocomposites, Journal of Non-Crystalline Solids. 357 (2011) 610–614. https://doi.org/10.1016/j.jnoncrysol.2010.06.058.

[21] P. Klonos, G. Dapei, I.Ya. Sulym, S. Zidropoulos, D. Sternik, A. Deryło-Marczewska, M.V. Borysenko, V.M. Gun'ko, A. Kyritsis, P. Pissis, Morphology and molecular dynamics investigation of PDMS adsorbed on titania nanoparticles: Effects of polymer molecular weight, European Polymer Journal. 74 (2016) 64–80. https://doi.org/10.1016/j.eurpolymj.2015.11.010.

[22]   P. Klonos, A. Kyritsis, L. Bokobza, V.M. Gun'ko, P. Pissis, Interfacial effects in PDMS/titania nanocomposites studied by thermal and dielectric techniques, Colloids and Surfaces A: Physicochemical and Engineering Aspects. 519 (2017) 212–222. https://doi.org/10.1016/j.colsurfa.2016.04.020.

[23]   J. Van Alsten, Experimental measurements of local mobility in adsorbed poly(dimethylsiloxane) layers, Macromolecules. 24 (1991) 5320–5323. https://doi.org/10.1021/ma00019a017.

[24]   M. Zeghal, P. Auroy, B. Deloche, Local Uniaxial Order in a Grafted Polymer Melt via Deuterium NMR, Phys. Rev. Lett. 75 (1995) 2140–2143. https://doi.org/10.1103/PhysRevLett.75.2140.

[25]   M. Zeghal, B. Deloche, P.-A. Albouy, P. Auroy, Chain-segment order and dynamics in a grafted polymer melt: A deuterium NMR study, Phys. Rev. E. 56 (1997) 5603–5614. https://doi.org/10.1103/PhysRevE.56.5603.

[26]   M. Zeghal, B. Deloche, P. Auroy, Chain Segment Ordering in Swollen Polymer Brushes: Deuterium NMR Investigations, Macromolecules. 32 (1999) 4947–4955. https://doi.org/10.1021/ma981153y.

[27]   V.M. Litvinov, H. Barthel, J. Weis, Structure of a PDMS Layer Grafted onto a Silica Surface Studied by Means of DSC and Solid-State NMR, Macromolecules. 35 (2002) 4356–4364. https://doi.org/10.1021/ma0119124.

[28]   M. Wang, M. Bertmer, D.E. Demco, B. Blümich, V.M. Litvinov, H. Barthel, Indication of Heterogeneity in Chain-Segment Order of a PDMS Layer Grafted onto a Silica Surface by 1H Multiple-Quantum NMR, Macromolecules. 36 (2003) 4411–4413. https://doi.org/10.1021/ma0217534.

[29]   J.S. Smith, O. Borodin, G.D. Smith, E.M. Kober, A molecular dynamics simulation and quantum chemistry study of poly(dimethylsiloxane)–silica nanoparticle interactions, Journal of Polymer Science Part B: Polymer Physics. 45 (2007) 1599–1615. https://doi.org/10.1002/polb.21119.

[30]   P. Klonos, K. Kulyk, M.V. Borysenko, V.M. Gun'ko, A. Kyritsis, P. Pissis, Effects of Molecular Weight below the Entanglement Threshold on Interfacial Nanoparticles/Polymer Dynamics, Macromolecules. 49 (2016) 9457–9473. https://doi.org/10.1021/acs.macromol.6b01931.

[31]   P.A. Klonos, L.V. Nosach, E.F. Voronin, E.M. Pakhlov, A. Kyritsis, P. Pissis, Glass Transition and Molecular Dynamics in Core–Shell-Type Nanocomposites Based on Fumed Silica and Polysiloxanes: Comparison between Poly(dimethylsiloxane) and Poly(ethylhydrosiloxane), J. Phys. Chem. C. 123 (2019) 28427–28436. https://doi.org/10.1021/acs.jpcc.9b07247.